

Observation of Depolarized ZnO(0001) Monolayers: Formation of Unreconstructed Planar Sheets

C. Tusche,* H.L. Meyerheim, and J. Kirschner

Max-Planck-Institut für Mikrostrukturphysik, Weinberg 2, D-06120 Halle, Germany

(Received 21 February 2007; published 13 July 2007)

A novel nonpolar structure of 2 monolayer (ML) thick ZnO(0001) films grown on Ag(111) has been revealed, using surface x-ray diffraction and scanning tunneling microscopy. Zn and O atoms are arranged in planar sheets like in the hexagonal boron-nitride prototype structure. The observed depolarization is accompanied by a significant lateral 1.6% expansion of the lattice parameter and a 3% reduced Zn-O bond length within the sheets. The nonpolar structure stabilizes an atomically flat surface morphology unseen for ZnO surfaces thus far. The transition to the bulk wurtzite structure occurs in the 3–4 ML coverage range, connected to considerable roughening.

DOI: 10.1103/PhysRevLett.99.026102

PACS numbers: 68.35.Bs, 61.10.-i, 68.37.Ef, 68.47.Gh

Ionic crystals are abundant in nature, and their thin film analogs have attracted considerable research interest in different fields like in spintronics [1] and catalysis [2]. An important subclass are crystals exhibiting polar (so called Tasker type III) surfaces [3,4], which are intrinsically unstable due to the divergence of the electrostatic energy. The stability is restored by canceling the macroscopic dipole moment. For instance, a $p(2 \times 2)$ reconstruction is found to stabilize the (111) surface of oxides with bulk rock-salt structure as in the case of NiO and MgO [5], while a defect structure was observed by scanning tunneling microscopy (STM) and by surface x-ray diffraction (SXR) in the case of the (0001) and (000 $\bar{1}$) crystal surfaces of ZnO [6–8].

While depolarization mechanisms for bulk crystal surfaces have been explored in the past quite extensively, those acting in thin films, only a few monolayers (ML) thick, are almost unknown. In general, ultrathin films are characterized by a significant amount of under-coordinated atoms, and their arrangement is not confined by back-bonding to the underlying bulk. Consequently, atomic structures and depolarization mechanisms distinctly different from those of the bulk can be expected.

Considerable effort was invested in order to artificially stabilize reconstruction-free, but polar surfaces in thin ionic films. Such systems would constitute a new class of materials, unavailable in nature, and might be promising candidates for model catalysts. Experimentally, isolated islands of NaCl(111) [9] or MgO(111) [10] films were reported to preserve a bulklike termination, tentatively based on the absence of a superstructure. In contrast, recent theoretical studies dealing with freestanding MgO(111) [11] and ZnO [12,13] films suggest that thin oxide films adopt a nonpolar sheetlike arrangement. Despite the theoretical predictions and their great importance for thin film stabilization, no crystallographic analysis has been carried out thus far.

To this end, we have carried out a SXR and STM study of 2–5 ML thick ZnO films deposited on Ag(111). While

in the bulk wurtzite structure, Zn and O atoms are arranged in layers separated by a vertical distance of 0.63 Å, we find giant vertical inward relaxations of the Zn atoms into the plane of O atoms leading to an almost perfect depolarization. For the first time, compelling evidence is provided that ZnO adopts a hexagonal boron-nitride (*h*-BN)-like structure [14] in which Zn and O atoms are arranged in a trigonal-planar coordination instead of the bulk tetrahedral configuration. The SXR analysis supports previous theoretical predictions [12,13] and explains the appearance of an atomically flat surface morphology, distinctly different from those seen in the case of the bulk ZnO surfaces [6,7]. The transition to the bulklike wurtzite structure, which is accompanied by surface roughening, sets in between 3 and 4 MLs.

The STM and SXR [15] experiments were carried out in ultra high vacuum (UHV) at a base pressure of $\approx 1 \times 10^{-10}$ mbar. The Ag(111) single crystal ($\varnothing = 10$ mm) was cleaned by mechanical polishing, and *in situ* by cycles of Ar⁺ sputtering followed by annealing at 750 K until STM indicated terraces several 100 nm wide. ZnO was grown by pulsed laser deposition at 300 K using a stoichiometric target at a rate of 0.10 ML/s under an oxygen background pressure of 5×10^{-7} mbar. After annealing up to 680 K, stoichiometric films were formed as verified by x-ray photoelectron spectroscopy.

X-ray reflections were collected *in situ* using a five-circle diffractometer. Cu- K_{α} radiation from a rotating anode x-ray generator was focused by a multilayer x-ray optics on the sample surface under total reflection conditions (angle of incidence, $\alpha_i = 0.3^{\circ}$). Integrated intensities [16] were collected by rotating the sample about its surface normal, and structure factor intensities, $|F|^2$, were derived after correction for geometric factors [17].

An STM image of a 2.2 ML ZnO film is shown in Fig. 1(a). The film morphology is characterized by an atomically flat ZnO double-layer and by some third layer triangular islands, whose edges are aligned along high symmetry directions. Unlike bulk crystal surfaces, the

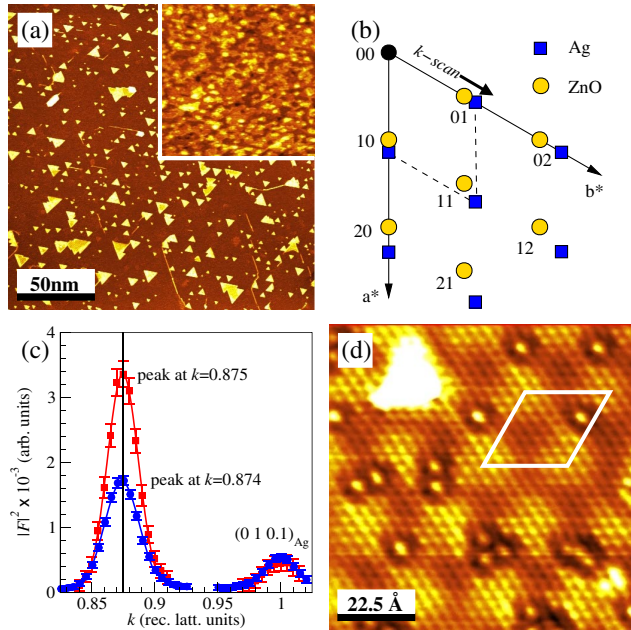


FIG. 1 (color online). (a) $200 \times 200 \text{ nm}^2$ STM image (+1.6 V bias/0.5 nA setpoint) of 2.2 ML ZnO on Ag(111). The inset shows 3.2 ML on the same scale. (b) Asymmetric unit in the $\vec{a}^*-\vec{b}^*$ -plane of the reciprocal space. The positions of Ag and ZnO reflections are marked by symbols. (c) Intensity along the \vec{b}^* axis [as indicated by k -scan in (b)]. (d) High resolution $9 \times 9 \text{ nm}^2$ STM image of the 2.2 ML film (+1.2 V/0.2 nA).

two ML thick film is atomically flat on a length scale only limited by the width of substrate terraces. The inset in Fig. 1(a) shows a thicker (3.2 ML) ZnO film on the same lateral scale. As compared to the 2.2 ML sample, the 3.2 ML surface is considerably rougher with several incomplete layers forming small ($\approx 10 \text{ nm}$ wide) islands.

The SXRD analysis provides the details of the coverage dependent evolution of the atomic film structure. The location of reflections within the $\vec{a}^*-\vec{b}^*$ -plane of the reciprocal space is outlined in Fig. 1(b): The in-plane lattice vectors of the ZnO film are aligned parallel to those of the Ag(111) surface unit cell [we use the hexagonal setting of the (111) surface], but the ZnO reflections are located at a lower in-plane momentum transfer than the corresponding ones of the Ag-lattice.

The intensity measured along the \vec{b}^* -axis is plotted (symbols) together with Gaussian profiles (lines) in Fig. 1(c) for an in-plane scattering geometry: The perpendicular momentum transfer $q_z = \ell c^*$ was fixed at $\ell = 0.1$, while the scan interval along the \vec{b}^* -axis extends from 0.82 to 1.02 reciprocal lattice units as indicated by k -scan in panel (b).

The substrate reflection is located at $k = 1$, while the first order reflection of the 2.7 ML (circles) and the 3.5 ML (squares) ZnO film is located at $k = 0.874(1)$ and $k = 0.875(1)$, respectively. Within the error bars, this corresponds to a 7/8 coincidence structure between ZnO and

the Ag(111) substrate. The ZnO peak positions indicate a lateral film relaxation: The lattice parameter, $a_{\text{ZnO}} = 3.303(2) \text{ \AA}$, is by 1.6% larger as compared to the bulk (3.249 \AA), independent of the film thickness.

The coincidence lattice of 7 ZnO to 8 Ag(111) surface unit cells is reflected in a Moiré type pattern in the high resolution STM topograph shown in Fig. 1(d). The topographic corrugation within the coincidence cell (indicated by the parallelogram) is attributed to the different position of Zn and O atoms with respect to the Ag substrate atoms. In addition to the Moiré pattern, the short period contrast between individual ZnO unit cells is observed, and the surface is atomically flat with only some isolated defects.

The three-dimensional structure of the ZnO film is derived from the quantitative analysis of structure factor intensities, $|F|^2$. While diffraction occurs at integer reciprocal space coordinates (hkl) in the bulk, the lack of periodicity along the surface normal leads to rods of intensity perpendicular to the surface. Consequently, the component of the perpendicular momentum transfer, ℓ , is a continuous parameter.

In the following, the indices h and k are given in units of the (1×1) ZnO reciprocal lattice, and ℓ in units of the Ag(111) c^* -axis ($a^* = b^* = 1.902 \text{ \AA}^{-1}$ and $c^* = 0.888 \text{ \AA}^{-1}$). Structure factor intensities were collected along three symmetry independent rods, namely, (10ℓ) , (11ℓ) , and (20ℓ) with $0.1 \leq \ell \leq 3.5$. They are displayed for the 2.7 ML and the 3.5 ML sample in Fig. 2(a)–2(c)

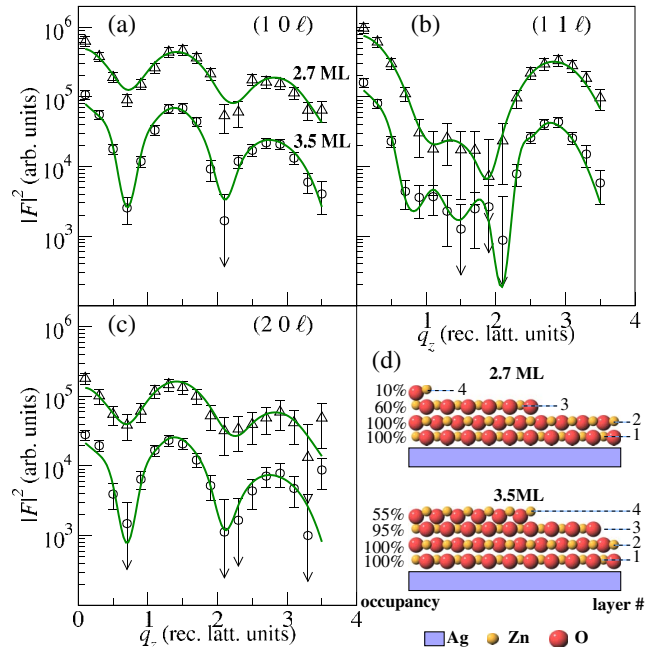


FIG. 2 (color online). (a)–(c) Measured (symbols) and calculated (lines) structure factor intensities, $|F_{hkl}|^2$, of 2.7 and 3.5 ML thick ZnO, as indicated by the labels at the (10ℓ) rod. Curves are shifted vertically for clarity. (d) Schematic structure models with layer fillings given in percent.

(symbols) together with calculated values (lines). The latter were obtained by a least squares fit leading to the structure models schematically sketched in Fig. 2(d). The fits almost perfectly agree with the measured data and reproduce all details, even at low intensities. Quantitatively, this is expressed by a goodness of fit (GOF) [18] of 0.90 and 0.97, respectively. Other samples measured (not shown) yield a GOF = 0.82 for 3.0 ML and GOF = 0.94 for 4.5 ML ZnO.

The (1×1) ZnO unit cell is the basic building block of the film structure. It consists one Zn and one O atom placed at the relative lateral positions $(x, y) = (1/3, 2/3)$ and $(2/3, 1/3)$, alternating layer by layer. Apart from the overall scale factor, only the z -coordinates of the atoms and the fractional layer filling, representing incomplete layers, need to be refined. The bulk 1:1 ZnO stoichiometry was kept fixed within all layers.

When more than 2 ML were deposited, two complete ZnO layers labeled by 1 and 2 are observed. The fractional occupancy of each layer is schematically represented by the number of solid spheres, and the layer numbers are indicated on the right hand side of panel (d), beginning with the bottom ZnO layer. The experimentally determined layer profile indicates a sharp interface to the Ag(111) substrate. Interface intermixing and roughening was observed at annealing temperatures above 750 K. With increasing coverage, layers 3 and 4 do not become completely filled before the next layer is occupied. They are not completed even at 4.5 ML (not shown), the largest thickness studied. The fraction of incomplete layers at film thicknesses beyond 2.0 ML agrees with the observation by STM, e.g., for the 3.2 ML sample in Fig. 1(a). The film corrugation observed by STM is reflected by a twice larger out-of-plane component of the Debye-parameter as compared to the in-plane component. The z -modulation of the atoms is determined to be 0.2–0.3 Å root mean square.

The SXRD analysis provides evidence for several structural modifications. In detail: (i) As pointed out above, the in-plane lattice constant is expanded by +1.6% relative to the bulk. (ii) Distances d_{nm} between the Zn atoms in layers n and m are represented in Fig. 3(a) by different symbols for samples with thicknesses ranging from 2.7 to 4.5 ML. Error bars are in the ± 0.1 Å range estimated on the basis of the variance of the agreement factors and the scatter of the results derived from independent experiments. Based on the layer resolved structure parameters derived from the averaging over the four independent data sets (see solid lines), we find that the spacing d_{12} is contracted by -11% with respect to the bulk (2.60 Å), but the second and third interlayer distance, d_{23} and d_{34} , already approach the bulk value. (iii) Fig. 3(b) shows the vertical oxygen coordinate, u_n , in layer number n . The parameter u represents the height difference between the Zn and O atom within a given layer. In the bulk wurtzite structure, u equals to 0.63 Å, as marked by the dashed line, but is strongly

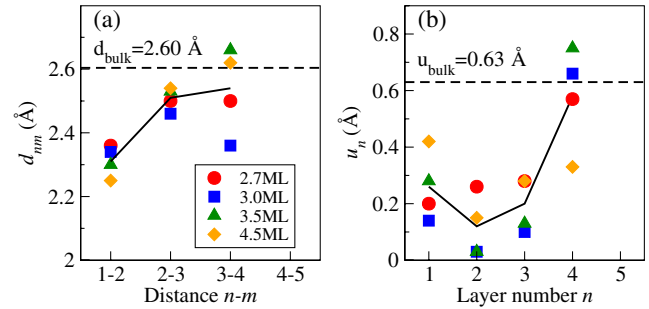


FIG. 3 (color online). Distance, d_{nm} , between layer number n and m (a) and the oxygen coordinate, u_n , in layer number n (b) for samples between 2.7 and 4.5 ML thickness. The solid line represents the average value, and the dashed lines indicate the corresponding bulk values.

reduced in the layers 1, 2, and 3. The lowest value is determined for layer number 2, where we find $u_2 = 0.12 \pm 0.10$ Å, corresponding to only 19% of the bulk.

The small parameter u observed is indicative for a significant depolarization of the structure. The polarity is restored in layer 4, in which u_4 is bulklike. This nicely correlates with the onset of surface roughening observed by STM in the inset of Fig. 1(a). It thus can be concluded that at this coverage, the transition to a bulklike stabilization of the surface sets in.

The relaxations of the bottom layers substantially modify the geometric arrangement. For a comparison, the bulk (wurtzite-type) ZnO structure is shown in Fig. 4(a). It is characterized by Zn and O atoms in a tetrahedral coordination. The bond length within one layer is labeled by $d_{\text{Zn-O}}$, while the ZnO bond length between different layers is labeled by $d'_{\text{Zn-O}}$. In the bulk structure, *all* ZnO bond lengths equal to 1.98 Å.

Figure 4(b) shows the structure of the two ZnO layers next to the substrate (layers 1 and 2). The bulk structure is modified in the way that the Zn atoms almost completely relax into the plane of the O atoms. Consequently, Zn and O atoms adopt a planar threefold coordination like in the *h*-BN prototype structure, instead of the tetrahedral bulk one. Based on the average of all samples, $d_{\text{Zn-O}}$ shortens to

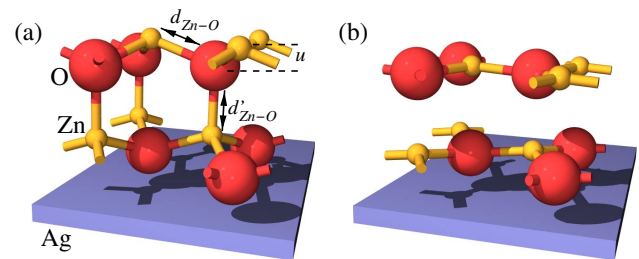


FIG. 4 (color online). The bulk ZnO (wurtzite) structure (a) and the experimentally derived structure model for the first two monolayers (b). Small and large balls represent Zn and O atoms, respectively.

TABLE I. Intra- ($d_{\text{Zn-O}}$) and interlayer ($d'_{\text{Zn-O}}$) bond length between Zn and O atoms, from the SXRD analysis. Individual error bars are $\pm 0.01 \text{ \AA}$ for $d_{\text{Zn-O}}$ and $\pm 0.10 \text{ \AA}$ for $d'_{\text{Zn-O}}$, calculated from the geometry and experimental values.

Coverage	$d_{\text{Zn-O}}$			$d'_{\text{Zn-O}}$	
	layer 1	layer 2	layer 3	layer 1–2	layer 2–3
2.7 ML	1.92 \AA	1.92 \AA	1.93 \AA	2.10 \AA	2.22 \AA
3.0 ML	1.91 \AA	1.91 \AA	1.91 \AA	2.31 \AA	2.36 \AA
3.5 ML	1.93 \AA	1.91 \AA	1.91 \AA	2.27 \AA	2.40 \AA
4.5 ML	1.95 \AA	1.91 \AA	1.93 \AA	2.10 \AA	2.26 \AA

$1.92 \pm 0.01 \text{ \AA}$; i.e., it is 3% smaller than in the bulk, while $d'_{\text{Zn-O}}$ increases by 11% to $2.20 \pm 0.10 \text{ \AA}$. The layer resolved bond lengths are summarized in Table I for the individual samples. There is some scatter between individual values, which however is not significant within the experimental error bars.

The shortening of $d_{\text{Zn-O}}$ and the expansion of $d'_{\text{Zn-O}}$ with respect to the bulk agrees with the theoretical predictions for unsupported films: A ZnO bond length of 1.93 \AA within the hexagonal plane and of $2.14\text{--}2.16 \text{ \AA}$ between planes was proposed in Ref. [13]. Although the *h*-BN structure is predicted to be favored up to 9 ZnO layers [12], we find a restored surface polarity already for the 4th layer [e.g., see Fig. 3(b)]. The difference might be attributed to the competition with the bulk stabilization mechanism involving structural defects and roughening [7], which were not considered in Ref. [12].

The excellent agreement between the structure model and the theory suggests that the Ag substrate has only a minor effect on the ZnO film structure. In particular, we conclude that the 1.6% expanded in-plane lattice parameter is close to the equilibrium value of a freestanding ZnO film. This conclusion is supported by considering the Ag/ZnO(0001) structure, i.e., the inverted system, in which the ZnO structure does not relax laterally [19]. There, a 9/8 coincidence is found in perfect agreement with the bulk lattice parameters (2.889 \AA and 3.249 \AA for Ag and ZnO, respectively) [19].

The in-plane expansion can be related to the formation of the *h*-BN like geometry: In a hard sphere model, the distance between the atoms is given by the sum of their radii, and an inward relaxation to the planar Zn-O arrangement involves an in-plane expansion. We may speculate that the “lock-in” into the 7/8 coincidence structure might be energetically favorable over an incommensurate structure in this way limiting the lateral expansion. This might account for the fact that the relaxation to the *h*-BN structure is not complete (i.e., $u \neq 0$).

In summary, the SXRD analysis of ultrathin ZnO (0001) films deposited on Ag(111) has provided direct evidence

for the presence of a *h*-BN like structure characterized by flat hexagonal ZnO sheets in which Zn and O atoms are threefold coordinated. Unlike in the *h*-BN prototype structure, some buckling remains, but is largely reduced as compared to bulk ZnO. This depolarization mechanism is very distinct from that known for the polar bulk crystal surface characterized by a defect structure. The formation of the planar structure is related to an atomically flat surface morphology, thus far unseen for ZnO surfaces. Our experimental findings support the recently proposed planar geometry in Refs. [11,12]. Similarly, the observed depolarization mechanism might be important for the structure of other thin oxide films and should be considered in future investigations.

This work is supported by the German Science Foundation (DFG) in the researchers group No. FOR404.

*tusche@mpi-halle.mpg.de

- [1] S. A. Chambers, T. C. Droubay, C. M. Wang, K. M. Rosso, S. M. Heald, D. A. Schwartz, K. R. Kittilstved, and D. R. Gamelin, *Mater. Today* **9**, 28 (2006).
- [2] M. Bäumer and H.-J. Freund, *Prog. Surf. Sci.* **61**, 127 (1999).
- [3] P. W. Tasker, *J. Phys. C* **12**, 4977 (1979).
- [4] C. Noguera, *J. Phys. Condens. Matter* **12**, R367 (2000).
- [5] F. Finocchi, A. Barbier, J. Jupille, and C. Noguera, *Phys. Rev. Lett.* **92**, 136101 (2004).
- [6] O. Dulub, L. A. Boatner, and U. Diebold, *Surf. Sci.* **519**, 201 (2002).
- [7] O. Dulub, U. Diebold, and G. Kresse, *Phys. Rev. Lett.* **90**, 016102 (2003).
- [8] N. Jedrecy, M. Sauvage-Simkin, and R. Pinchaux, *Appl. Surf. Sci.* **162–163**, 69 (2000).
- [9] W. Hebenstreit, M. Schmid, J. Redinger, R. Podlucky, and P. Varga, *Phys. Rev. Lett.* **85**, 5376 (2000).
- [10] M. Kiguchi, S. Entani, K. Saiki, T. Goto, and A. Koma, *Phys. Rev. B* **68**, 115402 (2003).
- [11] J. Goniakowski, C. Noguera, and L. Giordano, *Phys. Rev. Lett.* **93**, 215702 (2004).
- [12] C. L. Freeman, F. Claeysens, N. L. Allan, and J. H. Harding, *Phys. Rev. Lett.* **96**, 066102 (2006).
- [13] F. Claeysens, C. L. Freeman, N. L. Allan, Y. Sun, M. N. R. Ashfold, and J. H. Harding, *J. Mater. Chem.* **15**, 139 (2005).
- [14] The structure is of the boron-nitride type instead of the graphite type due to the different stacking of the sheets.
- [15] I. K. Robinson and D. J. Tweet, *Rep. Prog. Phys.* **55**, 599 (1992).
- [16] R. Feidenhans'l, *Surf. Sci. Rep.* **10**, 105 (1989).
- [17] E. Vlieg, *J. Appl. Crystallogr.* **30**, 532 (1997).
- [18] S. C. Abrahams, *Acta Crystallogr. Sect. A* **25**, 165 (1969).
- [19] N. Jedrecy, G. Renaud, R. Lazzari, and J. Jupille, *Phys. Rev. B* **72**, 195404 (2005).